JACS
JOURNAL OF THE AMERICAN CHEMICAL SOCIETY
Article
pubs.acs.org/JACS

From Bis(silylene) and Bis(germylene) Pincer-Type Nickel(II) Complexes to Isolable Intermediates of the Nickel-Catalyzed Sonogashira Cross-Coupling Reaction

Daniel Gallego,[†,§] Andreas Brück,[†,§] Elisabeth Irran,[†] Florian Meier,[†] Martin Kaupp,[†] Matthias Driess,*[,†] and John F. Hartwig*[,‡]

[†]Metalorganics and Inorganic Materials, Department of Chemistry, Technische Universität Berlin, Straße des 17, Juni 135, Sekr. C2, 10623 Berlin, Germany

[‡]Department of Chemistry, University of California−Berkeley, 718 Latimer Hall, Berkeley, California 94720, United States

Supporting Information

ABSTRACT: The first [ECE]Ni(II) pincer complexes with E = Si^{II} and E = Ge^{II} metallylene donor arms were synthesized via C−X (X = H, Br) oxidative addition, starting from the corresponding [EC(X)E] ligands. These novel complexes were fully characterized (NMR, MS, and XRD) and used as catalyst for Ni-catalyzed Sonogashira reactions. These catalysts allowed detailed information on the elementary steps of this catalytic reaction (transmetalation → oxidative addition → reductive elimination), resulting in the isolation and characterization of an unexpected intermediate in the transmetalation step. This complex, {[ECE]Ni acetylide → CuBr} contains both nickel and copper, with the copper bound to the alkyne π-system. Consistent with these unusual structural features, DFT calculations of the {[ECE]Ni acetylide → CuBr} intermediates revealed an unusual E−Cu−Ni three-center−two-electron bonding scheme. The results reveal a general reaction mechanism for the Ni-based Sonogashira coupling and broaden the application of metallylenes as strong σ-donor ligands for catalytic transformations.

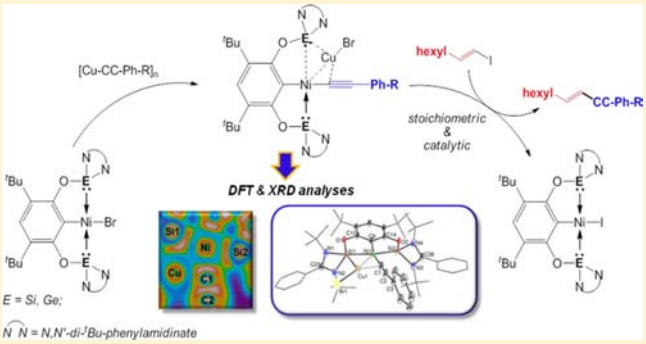

INTRODUCTION

Transition metal (TM) centers create a vast range of applications in organometallic chemistry, but the ligands control the reactivity of these sites. During the past decades, many ligands have been developed that have created a wide range of new reactivities. For example, the pincer-type motif [EDE], a tridentate, meridional coordinating ligand framework, offers a myriad of opportunities to fine-tune the steric and electronic properties of TM complexes.[1]

Generally, the arms (E) of a pincer ligand consist of neutral, two-electron Lewis donor moieties (e.g., E = PR_2, NR_2, or SR), which are connected over a linker group (often CH_2 or O) to the neutral or monoanionic anchoring site (D, e.g., a pyridyl or phenyl group). Highly electron-rich [PCP] pincer complexes of Ir have been applied to activate the strong bonds of ammonia[2] and alkanes,[3] and [PCP]Pd systems catalyze C−C coupling reactions.[4]

σ-Stabilized metallylene (silylene or germylene) donor ligands have also given rise to unique properties and reactivities.[5,6] It is noteworthy that bis-silylene and -germylene pincer moieties are more σ-donating than P^{III}-based ligands. This difference in σ donation was established through structural and spectroscopic investigation of the series of iridium olefin [ECE]IrHCl(coe) (E = Si, Ge, P) complexes.[7] In addition, the first experiments with the bis-silylene pincer arene **SiCHSi** and the group 10 metal precursor $Pd(PPh_3)_4$ led to the unexpected formation of a mixed silylene(Si^{II})−silyl(Si^{IV})−pincer Pd(II) complex (Scheme 1).[8] This unexpected result raised the question of whether isolable group 10 metal [ECE]M(II)X complexes (E = Si^{II}, Ge^{II}; X = halogen) with E: → M(II) ← :E coordination are at all accessible.

On the other hand, cross-coupling reactions are one of the most important breakthroughs in chemical synthesis,[9,10] although the catalytic pathways remain unclear and in rare cases reaction intermediates have been isolated.[9e,10b,f] Lately the Sonogashira reaction, normally catalyzed by Pd^0 species with CuI as cocatalyst (Figure 1), has been catalyzed using nickel-based catalysts.[10g,h] Nickel pincer complexes were recently reported to catalyze Sonogashira reactions[10] between a terminal alkyne and a sp^2 (or sp^3)[11] hybridized carbon electrophile (typically in the presence of a copper cocatalyst). The authors of the later work proposed that the catalytic cycle might involve a Ni^{II} → Ni^{IV} couple, but no experimental evidence for the formation of Ni^{IV} was gained. Therefore, it is important to gain access to intermediates that could reveal the connections

Received: August 9, 2013
Published: September 20, 2013

   dx.doi.org/10.1021/ja408137t | J. Am. Chem. Soc. 2013, 135, 15617−15626

Scheme 1. Earlier and Present Complexation Studies of ECXE Pincer Ligands toward Group 10 Metals

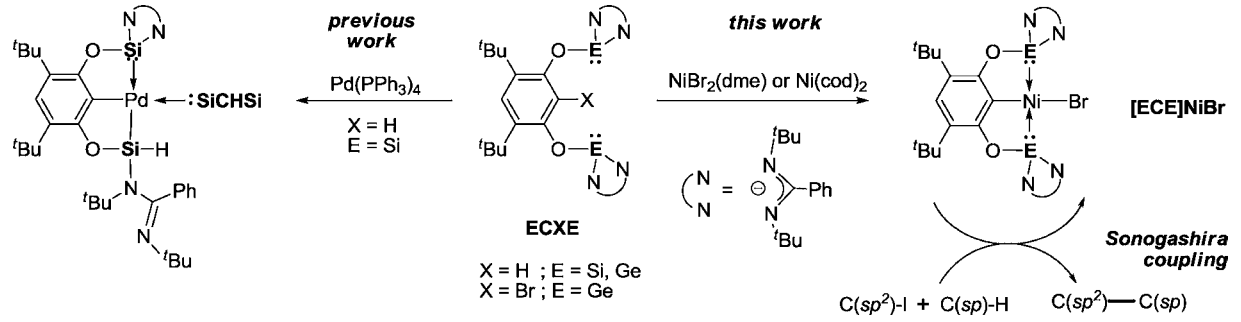

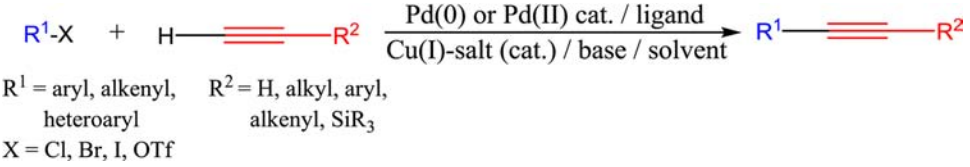

Figure 1. General conditions in Sonogashira cross-coupling.

between the structures of the intermediates and the rates and selectivity of the intermediates.

Herein, we report the synthesis of the novel bromo bis-germylene **GeCBrGe** pincer arene and the straightforward coordination chemistry of the **ECHE** (E= Si, Ge) and **GeCBrGe** ligands toward nickel, a nonprecious metal center. These studies led to the formation of [ECE]NiBr complexes, and these complexes catalyzed the Sonogashira coupling reaction (Scheme 1). Most important, reactions catalyzed by these strong σ-donor based pincer ligands enabled the isolation of elusive intermediates of the Sonogashira coupling. The results demonstrate for the first time that chemical transformations at a nonprecious metal center with pincer-like metallylene donor arms are viable processes.

RESULTS AND DISCUSSION

Synthesis of the GeCBrGe Pincer Ligand. From our previous metalation studies on the **SiCHSi** ligand with a group 10 TM using $Pd(PPh_3)_4$ as the metal source, we observed an unexpected formation of silylene(SiII)−silyl(Si^{IV})−pincer Pd(II) complex (Scheme 1).[8] This occurred through a hydride migration from the Pd(II)−H transient species to one of the silylene arms of the ligand. Therefore, we explored alternative routes to [ECE]MX complexes, avoiding the intermediacy of M−H bonds. In parallel, we sought to expand the coordination chemistry of these ligands to a nonprecious metal center (e.g., nickel) and explore their potential to increase the electron density on the metal for catalytic applications.

A common way to synthesize complexes bearing a $C(sp^2)$−M^{II}−X motif is the oxidative addition of a suitable M^0 precursor into a $C(sp^2)$−X bond. Consequently we envisioned preparing the nickel complexes of ECE pincer ligands from the reaction of ECBrE (E = Si, Ge) compounds with $Ni(cod)_2$ (cod = 1,5-cyclooctadiene) as a Ni^0 source. However, the synthesis of the ECBrE starting material was challenging, and only successful results were obtained for the **GeCBrGe** ligand. Slow addition of 2 molar equiv of LHMDS in toluene to a mixture of 2-bromo-4,6-di-*tert*-butylresorcinol and 2 molar equiv of the *N*,*N*′-di-*tert*-butylchloro(phenylamidinate)germanium(II) at room temperature produced a new species. The ^{1}H NMR spectrum of this compound contained two singlets for the *tert*-butyl groups with the relative ratio of 1:2. Purification by extraction with *n*-hexane and recrystallization produced the desired ligand **GeCBrGe** in 68% yield as a colorless solid (Figure 2). **GeCBrGe** was fully

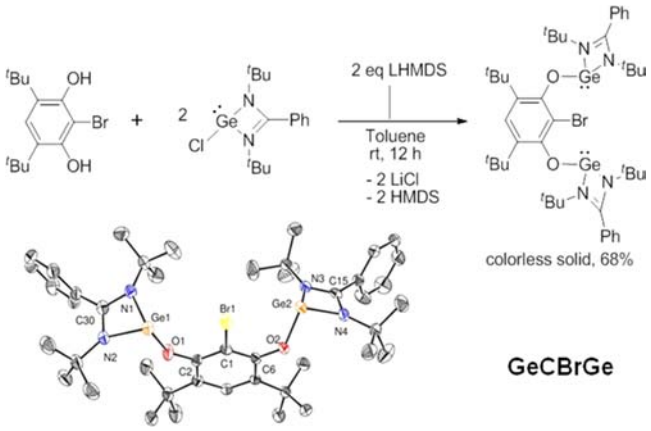

Figure 2. Synthesis and molecular structure of the novel **GeCBrGe** pincer ligand. Selected distances [Å] and angles [deg]: C1−Br1 1.905(3), O1−Ge1 1.862(2), O2−Ge2 1.868(2), C2−O1 1.347(3), C6−O2 1.355(3), Ge1−N1 2.031(3), Ge2−N4 2.021(2), C2−O1−Ge1 142.6(2), C6−O2−Ge2 136.3(2), N1−Ge1−N2 64.8(1), N3−Ge2−N4 64.8(1). Thermal ellipsoids are drawn at the 50% probability level. Hydrogen atoms are omitted for clarity. See Supporting Information for details.

characterized by ^{1}H and ^{13}C NMR, mass spectrometry, and single-crystal X-ray diffraction analysis (see Experimental Section and Supporting Information). Its structural features are similar to those of the GeCHGe ligand.[7] Reversing the addition sequence of the reactants led to the formation of an insoluble purple product of unknown composition. Unfortunately, attempts to obtain the silicon analogue **SiCBrSi** from the bromoresorcinol repeatedly led to undefined products.

Synthesis of [ECE]NiBr Complexes. The reaction of **GeCBrGe** with $Ni(cod)_2$ in toluene solution at −30 °C furnished a new species, as determined by ^{1}H NMR spectroscopy. The C_{2v} symmetry determined by the two singlets for the *tert*-butyl groups with the relative integral ratio of 1:2 and its mass spectrum ($M^{+\cdot}$, exptl 966.207 21 ; calcd

dx.doi.org/10.1021/ja408137t | J. Am. Chem. Soc. 2013, 135, 15617−15626

Scheme 2. Synthesis of the [ECE]NiBr Pincer-like Complexes (E = Si, Ge)

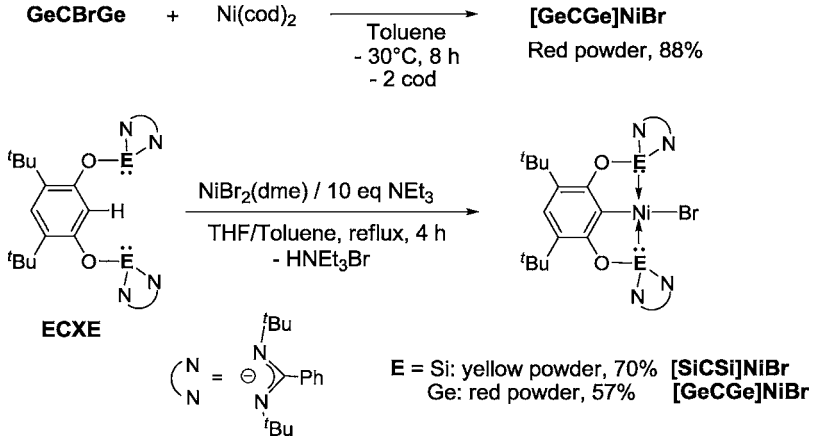

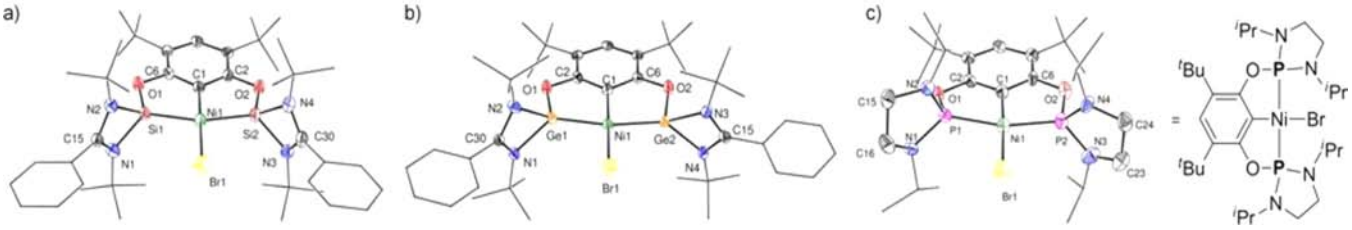

Figure 3. Molecular structures with selected distances [Å] and angles [deg]. (a) [**SiCSi**]**NiBr**: C1−Ni1 1.927(2), Br1−Ni1 2.3410(5), Si1−Ni1 2.1737(7), Si2−Ni1 2.1716(7), C1−Ni1−Br1 178.51(7), Si1−Ni1−Si2 161.75(3), C6−O1−Si1 110.8(1), C2−O2−Si2 110.5(1), Σ<Ni1 360.02(7). (b) [**GeCGe**]**NiBr**: C1−Ni1 1.961(3), Br1−Ni1 2.3351(5), Ge1−Ni1 2.2113(6), Ge2−Ni1 2.2190(6), C1−Ni1−Br1 178.5(1), Ge1−Ni1−Ge2 165.42(2), C2−O1−Ge1 109.9(2), C6−O2−Ge2 110.7(2), ∑∠Ni1 360.0(1). (c) [**PCP**]**NiBr**: C1−Ni1 1.881(4), Br1−Ni1 2.3297(7), P1−Ni1 2.136(2), P2−Ni1 2.151(2), C1−Ni1−Br1 178.0(2), P1−Ni1−P2 165.36(5), C2−O1−P1 111.6(3), C6−O2−P2 113.5(3), ∑∠Ni1 360.1(1). Thermal ellipsoids are drawn at the 50% probability level. Hydrogen and solvent atoms are omitted for clarity. See Supporting Information for details.

966.205 10) showed unambiguously the formation of the desired [**GeCGe**]**NiBr** pincer complex. This complex was isolated by extraction and recrystallization from *n*-hexane as a red powder in 88% yield (Scheme 2).

Because the silicon analogue could not be prepared by this route, we explored the possibility of synthesizing the pincer-type [**ECE**]**NiBr** complexes via reaction of the ECHE ligands (E = Si, Ge) with $NiBr_2$(dme) (dme = 1,2-dimethoxyethane). This reaction conducted with the **SiCHSi** ligand precursor in the presence of 10 mol equiv of NEt_3 in a refluxing THF/toluene solvent mixture led to change in color from dark blue to yellow within 4 h and with **GeCHGe** under the same conditions to a change in color from dark blue to dark red. The ^{1}H NMR spectroscopic investigation of the isolated Ni complexes showed the same features for the [**GeCGe**]**NiBr** complex obtained by oxidative addition of the C(sp^2)−Br bond described above. The absence of the phenyl C−H ^{1}H NMR resonance corresponding to the proton between the silylene donor arms and the sole resonance at δ = 20.2 ppm in the ^{29}Si{^{1}H} NMR spectrum of [SiCSi]NiBr are consistent with the formation of the desired pincer complex having a square-planar coordinated Ni(II) (Scheme 2). Single crystals suitable for additional characterization and structural elucidation by X-ray diffraction analysis were obtained for both complexes at ambient temperature in concentrated *n*-hexane solutions or by layering toluene solutions of [**SiCSi**]**NiBr** and [**GeCGe**]-**NiBr** with *n*-hexane, respectively (Figure 3).[12] Their molecular structures bearing square-planar Ni(II) sites were confirmed by X-ray diffraction analyses.

For direct comparison with the well-known phosphane pincer ligands, we prepared the analogous nickel complex containing the sterically and isoelectronically related P^{III}- pincer analogue PCHP.[7] Following the nickel metalation procedure for the ligands **ECHE** using $NiBr_2$(dme) (Scheme 2), the [**PCP**]**NiBr** complex was obtained in 95% yield (Figure 3c). Its ^{1}H NMR spectrum is consistent with a C_{2v} symmetric structure. This spectrum contained one doublet and one septet for the isopropyl group, and a single singlet resonance for the *tert*-butyl groups in a relative ratio of 12:2:9, as well as a singlet in the ^{31}P NMR spectrum at 134.6 ppm. This structural assignment was confirmed by X-ray diffraction analysis. As observed for the [**ECE**]**NiBr** complexes (E = Si, Ge), the Ni(II) sites have a square planar geometry (Figure 3c). By comparison of the bond distances in the crystal structures depicted in Figure 3, the E−Ni distances vary in accordance with the covalent radii of the donor atom. However, there is a slight difference in the Ni−Br distances depending on the donor atom E at the pincer arms [**ECE**]. The Ni−Br and C_{ipso}−Ni distances accordingy increased with the σ-donor strength of the ligand. This is in accordance with the order established previously for the same ligand series on the iridium(III) olefinic complexes [ECE]-IrHCl(coe) (E = P < Ge ≤ Si). The C−Ni bond is longer at about 5−8 pm for the complexes with Si and Ge as donors compared with the P^{III}-isoelectronic complex. Moreover, this effect is slightly lower for the Ni−Br bond distance where an increment of 1 pm is observable for the [**SiCSi**]**NiBr** complex.

Nickel-Catalyzed Sonogashira Cross-Coupling. We initially assessed the reactivity of the [**ECE**]**NiBr** pincer

dx.doi.org/10.1021/ja408137t | J. Am. Chem. Soc. 2013, 135, 15617−15626

complexes as catalyst for the Sonogashira reaction of (*E*)-1-iodo-1-octene with phenylacetylene as test substrates (Scheme 3). The reaction was conducted with 5 mol % of E = Si, Ge, and

Scheme 3. Evaluation of the [ECE]NiBr (E = Si, Ge, P) Complexes as Precatalysts in the Sonogashira Cross-Coupling Reaction

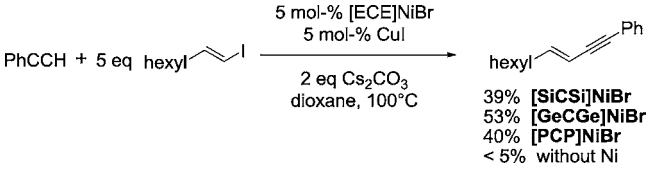

an excess of the halide substrate occurred in moderate yields. These yields are comparable to those of the isoelectronic P^{III}-based reference system [**PCP**]**NiBr**. The catalytic reaction mixtures with the [**ECE**]**NiBr** (E = Si, Ge, P) complexes turned dark to black, indicating the formation of Ni^0. This observation raised the question of whether the metallylene systems are stable under the reaction conditions and if the typical elementary steps of oxidative addition, transmetalation, and reductive elimination account for the catalytic activity. To the best of our knowledge, a defined chemical transformation at a metal center decorated with metallylene scaffolds has not been reported in the literature yet. This is of general interest, since metallylenes are prone to undergo chemical reactions with a great variety of functional groups.[5,6] Therefore, we explored stoichiometric reactions to identify possible intermediates of the Sonogashira reaction, including (i) transmetalation on the Ni(II) center with the copper acetylide, (ii) oxidative addition of the alkenyl iodide, and (iii) reductive elimination to produce the coupling product and regenerate the Ni(II) active species.

Stepwise Stoichiometric Reaction with Copper Acetylides. To investigate the first elementary step of the mechanism (i.e., transmetalation), copper phenylacetylide and the 4-methoxy and 3,5-bis-trifluoromethyl substituted derivatives were synthesized following the reported procedures.[13] The Cu acetylides are not soluble in either benzene or toluene, but 2 molar equiv reacted as a slurry with [**SiCSi**]**NiBr** in C_6D_6 over 3−4 h. NMR spectroscopic characterization of the reaction mixture after filtration through Celite showed that a new product with C_{2v} symmetry was formed. This symmetry was shown by one *tert*-butyl resonance in the ^{1}H NMR spectrum and one singlet resonance in the ^{29}Si{^{1}H} NMR spectrum (Scheme 4).

The products of this transmetalation were only moderately stable in solution for a couple of hours and gave a black precipitate upon evaporation of the solvent. The original signals for [**SiCSi**]**NiBr** reappeared partially in the ^{1}H NMR spectra and the homocoupled phenylacetylenes $(C{\equiv}C{-}Ph{-}R)_2$ were observed in GC−MS. These data indicate (i) that not all of the CuBr formed in the transmetalation could be removed by

Scheme 4. (i) Investigation of Possible Elementary Steps through Stoichiometric Transformations and (ii) Sequential ^{1}H and ^{29}Si NMR Spectra for the Course of the Coupling Reaction

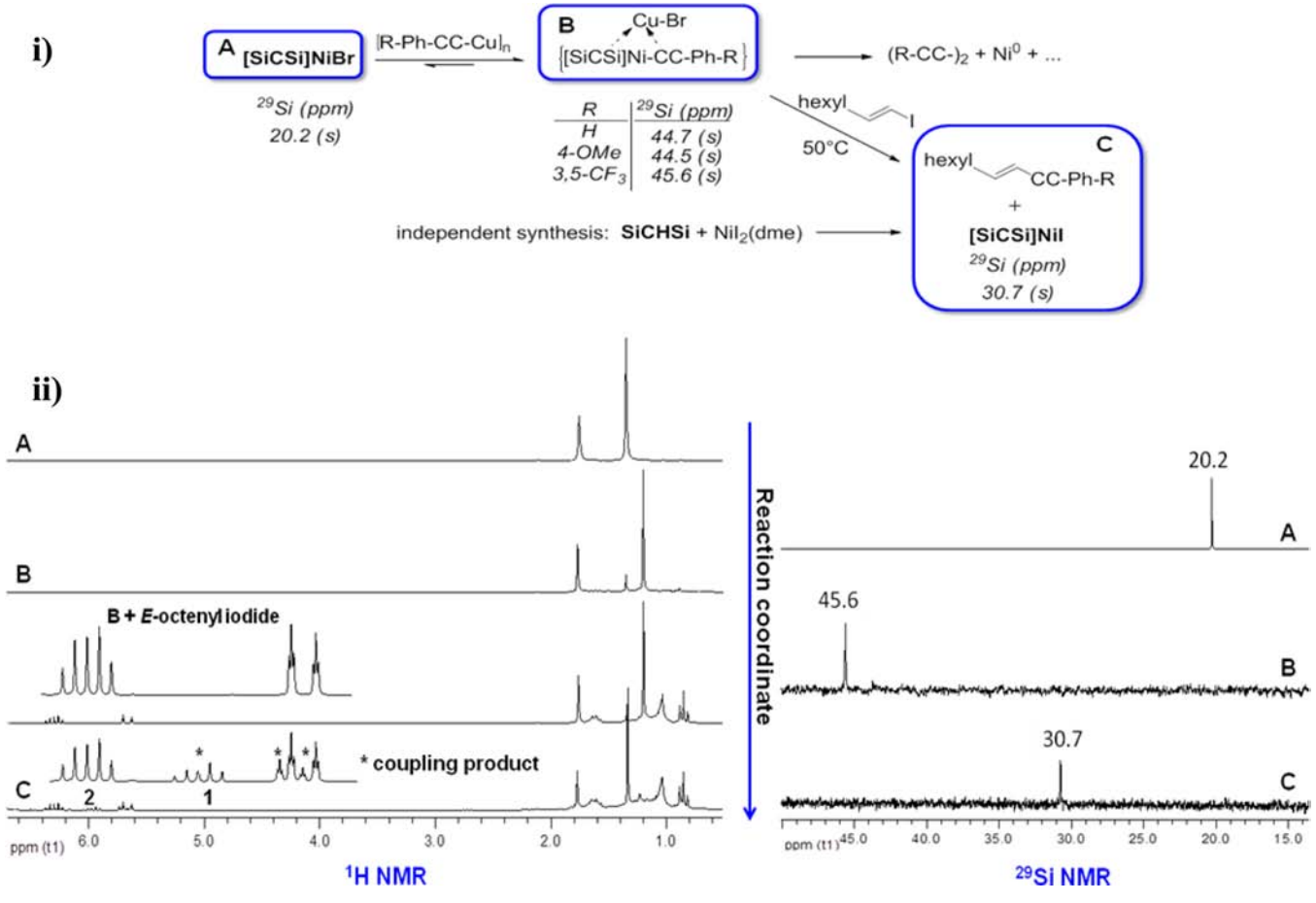

dx.doi.org/10.1021/ja408137t | J. Am. Chem. Soc. 2013, 135, 15617−15626

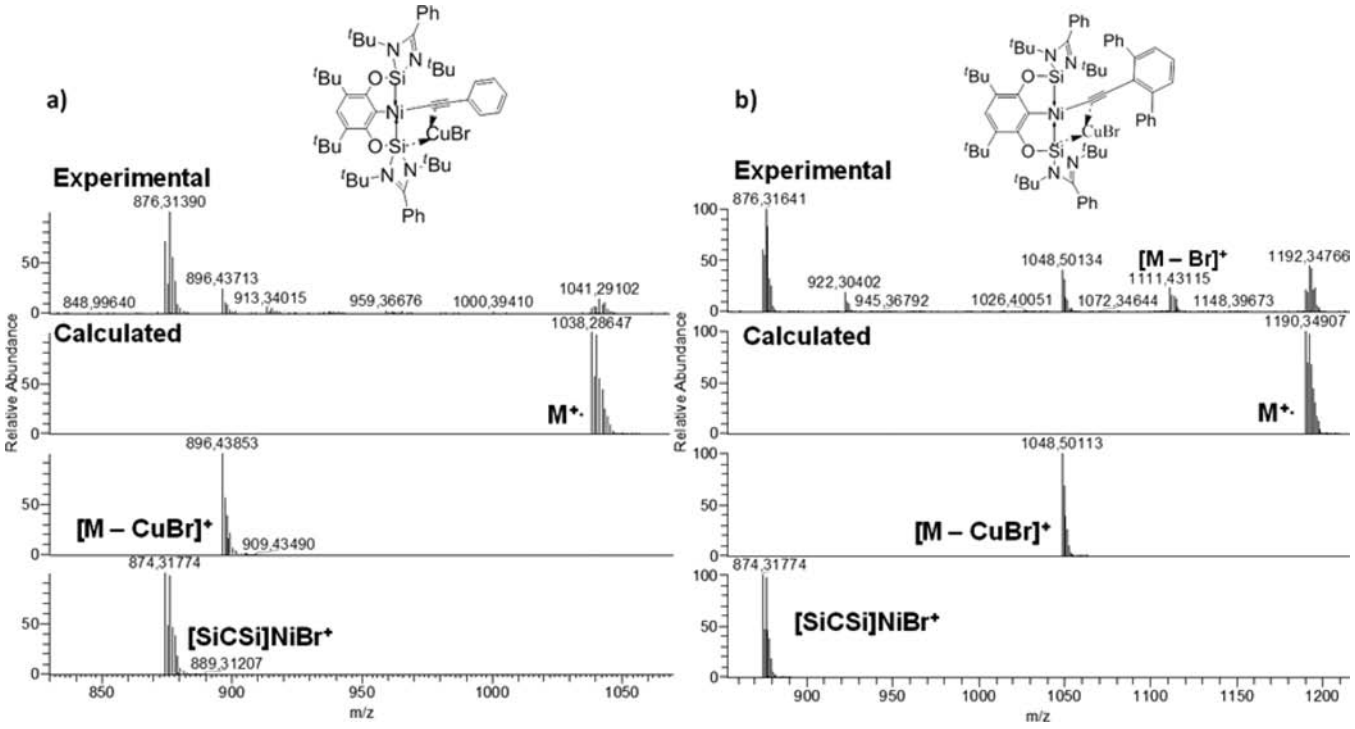

Figure 4. APCI-MS and calculated spectra for the transmetalation intermediates (a) {[**SiCSi**]**Ni**−**CC**−**Ph**→**CuBr**} and (b) {[**SiCSi**]**Ni**−**CC**−***ter*Ph**→**CuBr**}.

simple filtration and (ii) that the intermediate Ni acetylides (if formed) reacted in a bimolecular reaction to form the bis-acetylenes, Ni^0, and undefined organic products from the ligand.

To probe for a bimolecular decomposition pathway, the solutions generated by reaction of [**SiCSi**]**NiBr** with $[Cu{-}C{\equiv}C{-}Ph]_n$ and $[Cu{-}C{\equiv}C{-}3,5\text{-}(CF_3)_2Ph]_n$ were combined. The reaction products were analyzed by GC−MS after 1 day at room temperature. The mixed diyne Ph−C≡C−C≡C−3,5-$(CF_3)_2$Ph was detected. Further characterization of the crude Ni acetylides in solution by atmospheric pressure chemical ionization mass spectrometry (APCI-MS) showed three molecular ions in each case: [**SiCSi**]**NiBr** as the most intense signal, one signal for the expected Ni acetylides [SiCSi]Ni−C≡C−Ph−R, and one signal for an adduct {[SiCSi]Ni−C≡C−Ph−R→CuBr} (Figure 4a). The signals for the last two species were approximately equal in intensity.

Single crystals were obtained from the reaction of [**SiCSi**]-**NiBr** with $(Cu{-}CC{-}Ph)_n$ after microfiltration of the reaction mixture and storage in a mixture of *n*-pentane and toluene as solvent at −78 °C over approximately 1 week. Interestingly, the structure determined by X-ray diffraction corresponded to the {[**SiCSi**]**Ni**−**C**≡**C**−**Ph**→**CuBr**} adduct (Figure 5a). This structure consists of a copper center in proximity to the C≡C bond and the silylene unit (vide infra for a detailed discussion). Moreover, after redissolving the crystals in C_6D_6, the same mass spectrum with the three species and the symmetric NMR data as described above were obtained.

Transmetalation reactions between the synthesized Cu phenylacetylides and [**GeCGe**]**NiBr** occurred in a fashion similar to the reactions with [**SiCSi**]**NiBr**, but full conversion to the Ni phenylacetylide intermediates was not observed. However, the products were less stable and decomposed in the presence of larger quantities of the Cu phenylacetylides. The dependence of the stability of the transmetalation products on the amount of Cu phenylacetylide implies that at least one of the decomposition pathways of the Ni phenylacetylide complexes is bimolecular. Thus, we sought to sterically block the Ni center by conducting analogous reactions with a *m*-terphenylacetylide compound (Scheme 5).

Copper terphenylacetylide reacted cleanly with each of the metallylene pincer [**ECE**]**NiBr** (E = Si, Ge) complexes. As anticipated, the products were stable in solutions for several days without noticeable decomposition. The ^{1}H NMR spectrum of the bis-germylene derivative showed the same C_{2v} symmetry as described for the intermediates above, but the signals for the *tert*-butyl groups on the amidinate arms in the bis-silylene complex were broad singlets. This line shape could be due to (i) steric interactions between the silylene subunits and the terphenyl group or (ii) the reversible formation of an adduct with CuBr, thereby breaking the C_{2v} symmetry. The APCI-MS of the crude reaction contained three sets of signals for the [**ECE**]**NiBr** precursors, the [ECE]Ni−C≡C−*ter*Ph transmetalation product, and the CuBr adduct of the transmetalation product (the signal due to the adduct was more intense than it was for the nonsterically hindered acetylides, Figure 4b). This kinetic stabilization of the transmetalation product by steric hindrance allowed us to crystallize the copper acetylene adduct bound by the bis-germylene ligand at room temperature without any noticeable decomposition. The structure determined by X-ray diffraction data again revealed the formation of the adduct {[**GeCGe**]**Ni**−**C**≡**C**−***ter*Ph**→**CuBr**} (Figure 5b).

Transmetalation experiments with the phosphane analogue [**PCP**]**NiBr** with $[Cu{-}C{\equiv}C{-}Ph]_n$ and $[Cu{-}C{\equiv}C{-}terPh]_n$ showed similar reactivity to the [**ECE**]**NiBr** complexes. However, the equilibrium is strongly shifted to the starting Ni−Br complex (see Supporting Information for NMR and MS data) and no desired product could be isolated. Reaction with 5 molar equiv of $[Cu{-}C{\equiv}C{-}Ph]_n$ at 60 °C for 12 h furnished

dx.doi.org/10.1021/ja408137t | *J. Am. Chem. Soc.* 2013, 135, 15617−15626

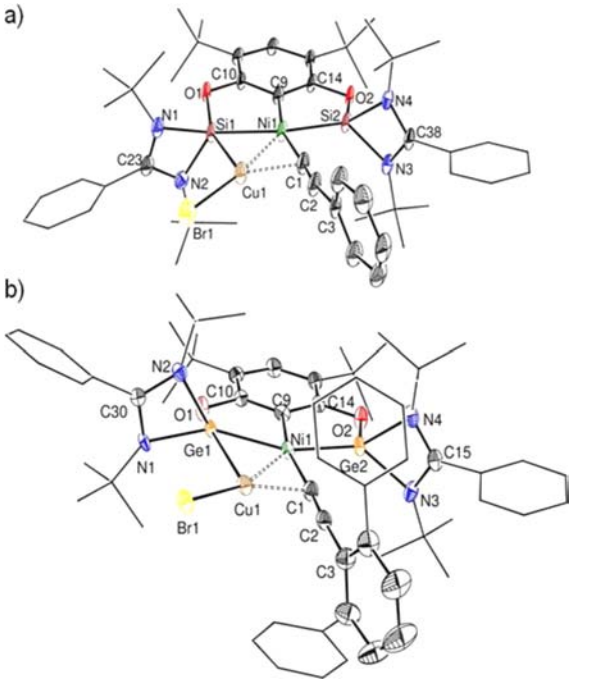

Figure 5. Molecular structures with selected bond lengths [Å] and angles [deg]. (a) {[**SiCSi**]**Ni−C≡C−Ph→CuBr**}: Ni1−Si1 2.296(1), Ni1−Si2 2.137(1), Ni1−C9 1.940(4), Ni1−C1 1.860(4), Ni1−Cu1 2.4628(9), Si1−Cu1 2.508(1),C1−Cu1 1.976(4), C2−Cu1 2.420(4), C1−C2 1.213(6), C2−C3 1.451(6), Cu1−Br1 2.2855(7), Si1−Ni1−Si2 160.93(5), C1−Ni1−C9 162.9(2), Ni1−Si1−Cu1 61.49(3), C10−O1−Si1 115.4(2), C14−O2−Si2 110.4(2), ∑∠Ni1 360.1(1). (b) {[**GeCGe**]**Ni−C≡C−*ter*Ph→CuBr**}: Ni1−Ge1 2.3254(6), Ni1−Ge2 2.1786(6), Ni1−C9 1.985(3),Ni1−C1 1.890(4), Ni1−Cu1 2.5208(7), Ge1−Cu1 2.5450(6),C1−Cu1 1.951(3), C2−Cu1 2.403(3), C1−C2 1.216(5), C2−C3 1.437(5), Cu1−Br1 2.2855(7), Ge1−Ni1−Ge2 161.09(3), C1−Ni1−C9 164.1(2), Ni1−Ge1−Cu1 62.15(2), C10−O1−Ge1 113.4(2), C14−O2−Ge2 109.0(2), ∑∠Ni1 360.4(1). Thermal ellipsoids are drawn at the 50% probability level. Hydrogen and solvent atoms are omitted for clarity. See Supporting Information for details.

Scheme 5. Synthesis of Kinetic Stabilized [ECE]Ni−C≡C−*ter*Ph→CuBr Intermediates

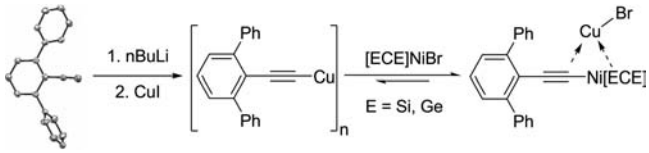

the transmetalation product in 5% conversion determined by ^{31}P NMR spectroscopy. Analysis by APCI-MS showed two molecular ion peaks for the [PCP]NiBr and [PCP]NiCCPh complexes, the latter with lower intensity. No CuBr adduct could be observed in this case. The difference in reactivity can be explained by the higher electron density at the Ni center in the [ECE]NiBr complexes which enables a stronger π-backbonding interaction with the C≡C bond, leading to a higher stability of the transmetalation product.[14]

Isolated Intermediates, Their Structural Features, and DFT Calculations. The coordination of the copper to the acetylide unit renders the structures in Figure 5 unsymmetrical. The **E−Ni** (E = Si, Ge) distances between the CuBr-coordinated side (d(Ni−Si1) = 2.296 Å, d(Ni−Ge1) = 2.325 Å) and the noncoordinated side (d(Ni−Si2) = 2.137 Å, d(Ni−Ge2) = 2.179 Å) are different in both {[**ECE**]**Ni−C≡C−Ph/*ter*Ph→CuBr**} complexes. In addition, the copper atom is much closer to the C1 atom (d(Cu−C1) = 1.976, 1.944 Å for E = Si, Ge, respectively) of the acetylide ligand than to the remote C2 atom (d(Cu−C2) = 2.420, 2.441 Å for E = Si, Ge, respectively). The unsymmetrical binding of the copper is different from a "classical side-on" coordination in which Δd(Cu−C1 vs Cu−C2) is less than 0.150 Å.[15] Additionally, the ∠(C1≡C2−C3) and ∠(Ni−C1≡C2) angles are indicative of a C≡C→Cu bond (side-on, about 156−165°; end-on, about 170−180°[15f,g]) and show, if at all, only minor perturbation of the C≡C bond (Si, 170.5° and 174.9°; Ge, 171.5° and 176.4°). The arms of the pincer ligands open toward the Cu atom in accordance with a reduction of the ∠(O1−E1−N) angles (average change: Si, 106.75° → 99.45°; Ge, 106.41° → 97.12°) and shortening of the Cu−E distances (d(Cu−Si) = 2.5080 Å; d(Cu−Ge) = 2.5704 Å), indicating a E→Cu bond.

To understand the bonding in the four member ring (C1−Ni−Si1−Cu), we conducted detailed density functional theory (DFT) calculations for both {[**ECE**]**Ni−C≡C−Ph/*ter*Ph→CuBr**} intermediates (E = Si, Ge) with B3LYP-D3(BJ)/def2-TZVP[16−18] functionals. For comparison, the corresponding [**ECE**]**Ni−C≡C−Ph/*ter*Ph** complexes lacking bound CuBr were also computed (see Experimental Section for computational details). Computations were conducted on (i) fully optimized structures (fullopt) and (ii) the X-ray crystal structures after reoptimization of the hydrogen-atom positions (crystal/H-opt). We focused mostly on atomic charges from natural population analysis (NPA) and on a real space description by the electron localization function (ELF)[19] or the related electron localizability indicator (ELI-D).[20] The bond distances of the fullopt structure agree well with those of the crystal/H-opt structure (Table 1). The main effect of CuBr coordination in all cases is lengthening of the **E1−Ni** bond and concomitant shortening of the **E2−Ni** bond opposite the CuBr fragment. Interestingly, the bending of the phenylacetylide ligand out of a straight C_{ipso}−Ni−C−C arrangement in both

Table 1. Selected Bond Lengths in Complexes {[ECE]Ni−CC−R→CuBr} and {[ECE]Ni−CC−R} (E = Si, R = Ph and E = Ge, R = *ter*Ph)[a]

	bond length [Å]					
	{[ECE]Ni−CC−R→CuBr}				{[ECE]Ni−CC−R}	
	crystal/H-opt[b]		fullopt-D3[b]		fullopt-D3[b]	
bond	E = Si	E = Ge	E = Si	E = Ge	E = Si	E = Ge
E1−Ni	2.296	2.317	2.319	2.329	2.181	2.199
E2−Ni	2.137	2.181	2.131	2.178	2.182	2.196
Ni−C1	1.861	1.881	1.866	1.885	1.848	1.858
C1−C2	1.212	1.219	1.233	1.232	1.222	1.224
C2−C3 (ipso, R[c])	1.452	1.444	1.420	1.423	1.413	1.414
Cu−C1	1.976	1.948	2.020	1.998		
Cu−C2	2.420	2.422	2.528	2.551		
Cu-E1	2.508	2.558	2.496	2.548		
Cu−Ni	2.462	2.526	2.485	2.531		
Cu−Br	2.286	2.285	2.318	2.306		

[a]For atom number assignment see Figure 5. [b]B3LYP/def2-TZVP results (cf. Computational Details). [c]C ipso of the phenylacetylide ligand.

dx.doi.org/10.1021/ja408137t | J. Am. Chem. Soc. 2013, 135, 15617−15626

complexes with CuBr is accompanied by a slight but significant lengthening of the alkyne triple bond and of the C2−C3 single bond.

The ELF plot displayed in Figure 6 shows that the Cu atom is involved in a three-center bond with **E1** and **Ni** (ELI-D gives

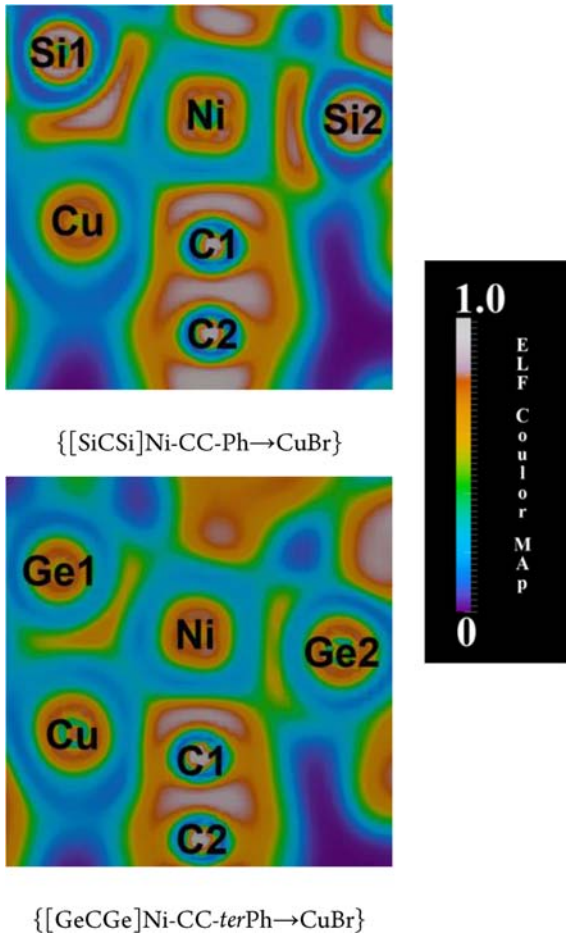

Figure 6. ELF plot in the main Ni coordination plane for {[**ECE**]**Ni**−**CC**−**Ph**/*ter***Ph**→**CuBr**} (E = Si, Ge) (B3LYP-D3/def2-TZVP level).

a qualitatively similar bonding description, Table S6 in Supporting Information). While no interaction of Cu with the acetylide ligand is apparent in the ELF, an appreciable **Cu**−**C1** Mayer bond order (Si, 0.963; Ge, 0.855) suggests that there are bonding interactions between Cu and the acetylide ligand (see Table S4 for further values). The reduced C≡C bond order in the full optimized structures containing the bound CuBr (Si, 0.728; Ge, 1.321), compared to the C≡C bond order in the system lacking CuBr (Si, 1.737; Ge, 2.076), is in agreement with a bonding interaction between C1 and the Cu center. NPA charges (Tables S2 and S3) show that CuBr receives about 0.2 electrons from the complex, and **E1** becomes more negative by about 0.18 electrons for E = Si and by about 0.13 electrons for E = Ge. Closer examination shows that this charge results mainly from **Ni** and the **E2** atom on the opposite side, with smaller contributions from other parts of the ligand framework. This charge distribution is consistent with a charge transfer toward the newly formed **E1**−**Cu**−**Ni** three-center bond (Figures 5 and 6). Overall, a pattern of delocalized interactions emerges that allows the CuBr fragment to bond to the combination of Ni, one metallylene arm from the pincer moiety, and the acetylide coligand.

After the complete analysis by the spectroscopic methods and DFT calculations of the {[**ECE**]**Ni**−**CC**−**Ph**/*ter***Ph**→**CuBr**} complexes, we conclude that the first step of the catalytic reaction occurs via a transmetalation process forming the CuBr adduct in solution with a medium half-life. Consequently, to study the next elementary step, the transmetalation products were generated in situ and used after microfiltration.

Stepwise Stoichiometric Reaction with (*E*)-1-Iodo-1-octene. One possible scenario for the observed Sonogashira coupling is the sequence of transmetalation, oxidative addition, and reductive elimination. In this sequence, oxidative addition of the substrate containing a C(sp^2)−halide bond would occur to the nickel acetylide. Indeed, addition of 3 molar equiv of (*E*)-1-iodo-1-octene to solutions of the in situ generated {[SiCSi]-Ni-phenylacetylides→CuBr} in C_6D_6 formed the C−C coupled products in yields from 80% to 95% (determined by GC/MS) after a few hours at 50 °C in combination with [**SiCSi**]**NiI** (Scheme 4). The spectroscopic features for the latter species were confirmed by the independent synthesis of the nickel iodide complex. This complex was prepared by the same procedure applied for the bromide analogue but using NiI_2(dme) as the metal precursor instead and fully characterized by ^{1}H and ^{29}Si NMR spectroscopies, APCI-MS, and X-ray analysis (see Experimental Section and Supporting Information for further details). The formation of the coupled product and the nickel iodide is consistent with a combination of oxidative addition and reductive elimination. The X-ray structure of [**SiCSi**]**NiI** resembles the structural features of [**SiCSi**]**NiBr**, concluding that no alteration on the ligand backbone has occurred after closing the catalytic cycle. At this stage, there is no evidence of the reaction intermediate for this elementary step. However, the perseverance of the *E* stereochemistry on the final product evidenced by ^{1}H NMR spectroscopy suggested the oxidative addition and subsequent reductive elimination as the most likely pathway.

Reaction Mechanism. The investigation of stoichiometric transformations reveals a general mechanism for the C−C coupling between phenylacetylene and (*E*)-1-iodo-1-octene catalyzed by [**ECE**]**NiBr** complexes (Scheme 6). The [ECE]-

Scheme 6. Proposed Catalytic Cycle

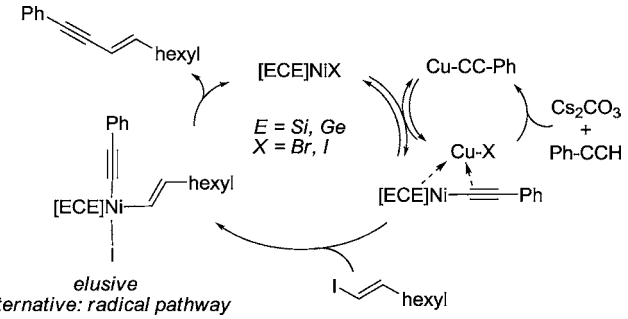

NiX (E = Si or Ge; X = Br or I) complex reacts with the Cu phenylacetylide generated in situ between the phenylacetylene and the CuI in the presence of Cs_2CO_3. The product of this transmetalation process binds CuBr to form the {[ECE]Ni−C≡C−Ph→CuBr} species. This species reacts with the alkenyl halide to form the organic product and to regenerate the nickel

dx.doi.org/10.1021/ja408137t | J. Am. Chem. Soc. 2013, 135, 15617−15626

halide. One possible sequence to form these products is oxidative addition and reductive elimination to form [**ECE**]**NiI** and (*E*)-dec-3-en-1-ynylbenzene.

CONCLUSIONS

In summary, the first silylene and germylene nickel pincer complexes [**ECE**]**NiBr** (E = Si, Ge) were synthesized by either a sequence of C−H activation and HBr elimination between **ECHE** and $NiBr_2$(dme) or C−Br oxidative addition of **GeCBrGe** by Ni(cod)$_2$. These novel structurally characterized complexes catalyze the Sonogashira coupling between phenylacetylene and (*E*)-1-iodo-1-octene to form (*E*)-dec-3-en-1-ynylbenzene. Most important, investigation of the proposed mechanism of this unusual nickel-catalyzed Sonogashira reaction by stoichiometric transformations allowed the isolation and structural characterization of a copper-bound nickel acetylide as the sole transmetalation product. This Ni(II) species reacts with alkenyl iodides (C(sp^2)−I) to form a Ni(II) iodide and the coupled product. These results suggest that the electron-rich nickel-pincer complexes with neutral Ge and Si donor atoms can react by a mechanism in which transmetalation precedes reaction with the haloarene. Moreover, the stoichiometric reaction raises the question of the oxidation state of the nickel intermediate that results from C−I bond cleavage and forms the C−C bond of the organic product. Further studies to elucidate the identity of such an intermediate are ongoing.

EXPERIMENTAL SECTION

General Considerations. All experiments and manipulations were conducted under dry oxygen-free nitrogen using standard Schlenk techniques or in a MBraun drybox with an atmosphere of purified nitrogen. Solvents were dried by standard methods and freshly distilled prior use. ^{1}H, ^{13}C, ^{31}P, and ^{29}Si NMR spectra were recorded on Bruker AV 400 (^{1}H, 400.13 MHz; ^{13}C, 100.61 MHz; ^{29}Si, 79.49 MHz) or AFM 200 (^{1}H, 200.13 MHz; ^{13}C, 50.32 MHz; ^{19}F, 188.33 MHz; ^{31}P, 81.01 MHz) spectrometers. The NMR signals are reported relative to the residual solvent peaks (^{1}H, $CDCl_3$, 7.26 ppm; C_6D_6, 7.15 ppm; ^{13}C, $CDCl_3$, 77.0 ppm; C_6D_6, 128.0 ppm) or an external standard (^{31}P, 85% H_3PO_4, 0.0 ppm; ^{29}Si, TMS, 0.0 ppm).

Single-Crystal X-ray Structure Determinations. Crystals were mounted on a glass capillary in perfluorinated oil and measured in a cold N_2 flow. The data were collected either on an Agilent Technologies Xcalibur S Sapphire at 150 K (Mo Kα radiation, λ = 0.710 73 Å) or an Agilent Technologies SuperNova (single source) at 150 K (Cu Kα radiation, λ = 1.5418 Å). The structures were solved by direct methods and refined on *F*2 with the SHELX-97 software package. The positions of the H atoms were calculated and considered isotropically according to a riding model. Mass spectra were recorded on a Finnigan MAT95S. IR spectra were recorded on a Perkin-Elmer Spectrum 100 FT-IR. GC−MS measurements were conducted on a Shimadzu GC-2010 gas chromatograph (30 m Rxi-5ms column) linked to a Shimadzu GCMA-QP 2010 Plus mass spectrometer. $NiBr_2$ and NiI_2 were purchased from Aldrich. $NiBr_2$(dme),[21] NiI_2(dme),[21] 2-bromo-4,6-di-*tert*-butylresorcinol,[22] and *N*,*N*′-di-*tert*-butylchloro(phenylamidinate)germanium(II)[23] were prepared according to the reported procedures, as well as the **SiCHSi**[11] and **GeCHGe**[10] and **PCHP**[10] ligands.

Synthesis of GeCBrGe. A solution of 2-bromo-4,6-di-*tert*-butylresorcinol (0.69 g, 2.3 mmol) in 20 mL of toluene was slowly added to a solution *N*,*N*′-di-*tert*-butylchloro(phenylamidinate)-germanium(II) (1.54 g, 4.5 mmol) in 20 mL of toluene at room temperature, forming a strong yellow reaction mixture. After the mixture was stirred for 30 min, a solution of LHMDS (0.77 g, 4.6 mmol) in 10 mL of toluene was added dropwise in a period of 30 min with concomitant formation of turbidity and color change to terracotta. All volatiles were removed in vacuo after stirring overnight at room temperature, and the product was extracted with hot hexane (1 × 60 mL, 2 × 20 mL) via cannula filtration. The product was concentrated up to 10 mL and crystallized overnight at −3 °C as white crystals. Further filtration and in vacuo drying produced 1.40 g of the desired product (68% yield). ^{1}H NMR (400.13 MHz, C_6D_6, 298 K): δ (ppm) = 1.07 (s, 36 H, NC(CH_3)$_3$), 1.83 (s, 18 H, ArC(CH_3)$_3$), 6.90−7.04 (m, 8 H, arom H), 7.29−7.32 (m, 2 H, arom H), 7.61 (s, 1 H, Ar-H). ^{13}C{^{1}H} NMR (100.61 MHz, C_6D_6, 298 K): δ (ppm) = 31.5 (ArC($\underline{C}H_3$)$_3$), 32.2 (NC($\underline{C}H_3$)$_3$), 35.8 (Ar$\underline{C}$(CH$_3$)$_3$), 53.1 (N$\underline{C}$(CH$_3$)$_3$), 111.6 (C_{arom}Br), 123.4 (C_{arom}H), 129.6 (C_{arom}*t*Bu), 127.4, 129.2, 129.9, 136.0 (C_{arom}H), 156.9 (C_{arom}O), 170.3 (N*C*N). APCI-MS (*m*/*z*): calcd for [$C_{44}H_{65}BrGe2N_4O_2^{\bullet+}$] 908.26975; found 908.26978 (correct isotope pattern). Elemental analysis for $C_{44}H_{65}BrGe_2N_4O_2$: calcd, C 58.25, H 7.22, N 6.18; found, C 58.45, H 7.35, N 6.18.

Synthesis of [ECE]NiX (E = Si, Ge, P; X = Br, I) Complexes. General Procedure with $NiBr_2$(dme). NEt_3 (10.0 equiv) was added to a suspension of $NiBr_2$(dme) (1.1 equiv) in THF, forming a dark blue solution. After the mixture was stirred for 20 min, a solution of **ECHE** (1.0 equiv) in toluene was added via cannula, and the reaction mixture was heated to reflux for 4 h. The mixture was allowed to cool to room temperature, filtered through a short plug of Celite, and all volatiles were removed in vacuo. The residue was extracted with hexane (1 × 50 mL, 2 × 20 mL) at 50 °C. The combined organic solutions were concentrated slowly in vacuo until small crystals formed at the glass wall. Further cooling in the freezer at −30 °C resulted in the crystallization of the pure products in the form of needles, which were collected by filtration and dried in vacuo for 2 h.

[SiCSi]NiBr. At 1.4 mmol scale: 70% yield; yellow needles. ^{1}H NMR (400.13 MHz, C_6D_6, 298K): δ (ppm) = 1.34 (s, 36 H, NC(CH_3)$_3$), 1.75 (s, 18 H, ArC(CH_3)$_3$), 6.79−6.91 (m, 8 H, CH_{arom}), 7.48 (s, 1 H, CH_{arom}), 7.69−7.71 (m, 2 H, CH_{arom}). ^{13}C{^{1}H} NMR (100.61 MHz, C_6D_6, 298 K): δ (ppm) = 30.8 (s, ArC($\underline{C}H_3$)$_3$), 31.5 (s, NC($\underline{C}H_3$)$_3$), 35.3 (s, Ar$\underline{C}$(CH$_3$)$_3$), 54.1 (s, N$\underline{C}$(CH$_3$)$_3$), 123.8 (s, CH_{arom}), 126.5 (s, $\underline{C}_{arom}$*t*Bu), 128.4 (s, CH_{arom}), 130.3 (s, 2C, CH_{arom}), 131.3 (s, $\underline{C}$Ni), 131.4 (s, C_{arom}), 162.7 (s, $\underline{C}_{arom}$O), 173.1 (s, N$\underline{C}$N). ^{29}Si{^{1}H} NMR (79.49 MHz, C_6D_6, 298 K): δ (ppm) = 20.22. APCI-MS (*m*/*z*): calcd for [$C_{44}H_{65}BrN_4NiO_2Si_2^{\bullet+}$] 874.317 74; found 874.318 05 (correct isotope pattern). Elemental analysis for $C_{44}H_{65}BrN_4NiO_2Si_2{\cdot}C_6H_{14}$: calcd, C 62.36, H 8.27, N 5.82; found, C 62.72, H 8.43, N 6.22.

[SiCSi]NiI. NiI_2(dme) was used as the precursor. At 0.3 mmol scale: 66% yield; orange needles. ^{1}H NMR (200 MHz, C_6D_6, 298 K): δ (ppm) = 1.33 (s, 36 H, NC(CH_3)$_3$), 1.77 (s, 18 H, ArC(CH_3)$_3$), 6.80−6.97 (m, 8 H, CH_{arom}), 7.54 (s, 1 H, CH_{arom}), 7.85−7.88 (m, 2 H, CH_{arom}). ^{13}C{^{1}H} NMR (50.32 MHz, C_6D_6, 298 K): δ (ppm) = 30.8 (s, ArC($\underline{C}H_3$)$_3$), 31.5 (s, NC($\underline{C}H_3$)$_3$), 35.4 (s, Ar$\underline{C}$(CH$_3$)$_3$), 54.1 (s, N$\underline{C}$(CH$_3$)$_3$), 123.9 (s, CH_{arom}), 126.6 (s, $\underline{C}_{arom}$^{t}Bu), 130.2 (s, CH_{arom}), 130.3 (s, CH_{arom}), 131.4 (s, C_{arom}), 135.7 (s, $\underline{C}$Ni), 162.5 (s, $\underline{C}_{arom}$O), 173.4 (s, N$\underline{C}$N). ^{29}Si{^{1}H} NMR (79.49 MHz, C_6D_6, 298K): δ (ppm) = 30.70. APCI-MS (*m*/*z*): calcd for [$C_{44}H_{65}IN_4NiO_2Si_2^{\bullet+}$] 922.303 87; found 922.303 96 (correct isotope pattern). Elemental analysis for $C_{44}H_{65}IN_4NiO_2Si_2$: calcd, C 57.21, H 7.09, N 6.06; found, C 56.44, H 6.47, N 7.17.

[GeCGe]NiBr. At 0.5 mmol scale: 57% yield; red needles. ^{1}H NMR (400.13 MHz, C_6D_6, 298 K): δ (ppm) = 1.21 (s, 36 H, NC(CH_3)$_3$), 1.83 (s, 18 H, ArC(CH_3)$_3$), 6.78−6.91 (m, 8 H, CH_{arom}), 7.06−7.10 (m, 2 H, CH_{arom}), 7.56 (s, 1 H, CH_{arom}). ^{13}C{^{1}H} NMR (100.61 MHz, C_6D_6, 298 K): δ (ppm) = 31.0 (s, ArC($\underline{C}H_3$)$_3$), 31.5 (s, NC($\underline{C}H_3$)$_3$), 35.8 (s, Ar$\underline{C}$(CH$_3$)$_3$), 54.4 (s, N$\underline{C}$(CH$_3$)$_3$), 125.1 (s, CH_{arom}), 125.4 (s, $\underline{C}_{arom}$C*t*Bu), 126.8 (s, C_{arom}), 128.7 (s, CH_{arom}), 128.7 (s, CH_{arom}), 130.0 (s, CH_{arom}), 132.3 (s, $\underline{C}$Ni), 162.6 (s, $\underline{C}_{arom}$O), 175.0 (s, N$\underline{C}$N). APCI-MS (*m*/*z*): calcd for [$C_{44}H_{65}BrGe_2N_4NiO_2^{\bullet+}$] 966.205 10; found 966.207 21 (correct isotope pattern). Elemental analysis for $C_{44}H_{65}BrGe_2N_4O_2$: calcd, C 54.71, H 6.78, N 5.80; found, C 54.22, H 7.06, N 5.51.

[PCP]NiBr. 95% yield, yellow needles. ^{1}H NMR (200.13 MHz, $CDCl_3$, 298 K): δ (ppm) = 1.31 (s, 18H, C(CH_3)$_3$), 1.32 (d, $^3J_{HH}$ = 6.6 Hz, 24 H, CH(CH_3)$_2$), 3.25−3.32 (m, 4H, CH_2), 3.33−3.39 (m, 4H, CH_2), 3.73−3.86 (m, 4H, CH(CH$_3$)$_2$), 6.93 (br s, 1H, CH_{arom}).

dx.doi.org/10.1021/ja408137t | J. Am. Chem. Soc. 2013, 135, 15617−15626

$^{13}C\{^1H\}$ NMR (50.32 MHz, $CDCl_3$, 298 K): δ (ppm) = 21.8 (t, $^2J_{CP}$ = 2.5 Hz, PC($\underline{C}H_3$)$_3$), 22.6 (t, $^2J_{CP}$ = 2.8 Hz, PC($\underline{C}H_3$)$_3$), 29.9 (s, ArC($\underline{C}H_3$)$_3$), 43.5 (s, CH_2), 47.1 (t, $^2J_{CP}$ = 7.1 Hz, P$\underline{C}$(CH$_3$)$_3$), 123.8 (s, CH_{arom}), 126.2 (t, $^3J_{CP}$ = 5.7 Hz, C_{arom}), 134.2 (t, $^1J_{CP}$ = 24.7 Hz, CNi), 156.5 (t, $^2J_{CP}$ = 13.2 Hz, CO). $^{31}P\{^1H\}$ NMR (81.01 MHz, $CDCl_3$, 298 K): δ (ppm) = 134.6 (s). HR-EI-MS (m/z): calcd for $[C_{30}H_{55}BrN_4NiO_2P_2^{\bullet+}]$ 704.231 66; found 704.177 70 (correct isotope pattern).

Procedure with GeCBrGe and Ni(cod)$_2$. Ni(cod)$_2$ (0.15 g, 0.53 mmol) was dissolved in 20 mL of toluene at −30 °C. A solution of **GeCBrGe** (0.53 g, 0.58 mmol) in 20 mL of toluene was added dropwise through a syringe. The stirred reaction mixture was slowly warmed to room temperature over the course of 8 h, resulting in a dark red solution, which was filtered. All volatiles from the filtrate were removed in vacuo, and the solid was washed with cold hexane (2 × 10 mL). The residue was dried in vacuo for 2 h, obtaining **[GeCGe]NiBr** as a dark red powder (0.45 g, 88% yield).

Catalytic Sonogashira Cross-Coupling. In a nitrogen filled drybox, [ECE]NiBr (5 mol %, 11.4 μmol), CuI (1.1 mg, 5 mol %, 11.4 μmol), Cs_2CO_3 (74.0 mg, 228.0 μmol), phenylacetylene (11.6 mg, 114 μmol), and (*E*)-1-iodooct-1-ene (1−5 equiv) were weighed into a 4.0 mL screw cap vial containing a stir bar and dissolved in 1.5 mL of 1,4-dioxane. The sealed vial was removed from the drybox and heated to 100 °C for 24 h in a temperature controlled heating block. After cooling, the mixture was filtered through a short plug of silica and all volatile materials were evaporated in vacuo. The yields of the products were determined by redissolving the crude product in $CDCl_3$ and adding a defined amount of CH_2Br_2 as internal reference and/or by addition of a defined amount of dodecane as internal standard to the reaction mixture before heating and taking small aliquots for analysis by GC−MS.

Stoichiometric Reactions with Copper Acetylides. In a nitrogen filled drybox, [ECE]NiBr (0.02−0.07 mmol) and [Cu−CC−Ph−R] (0.03−0.09 mmol) were weighted into a Schlenk flask or in a capped vial containing a stir bar and dissolved in the appropriate solvent (toluene or C_6D_6). The sluggish reaction mixture was stirred for 4 h and filtered through a short plug of Celite. Suitable crystals of {[SiCSi]Ni−CC−Ph→CuBr} for X-ray analysis were grown at −78 °C after several microfiltrations in a solvent mixture of *n*-pentane and toluene (1:1). For the complex {[GeCGe]Ni−CC-*ter*Ph→CuBr} the crystals were grown layering *n*-pentane on the toluene solution at room temperature.

Quantum Chemical Calculations. Computational Details. All structures were optimized at the B3LYP/def2-TZVP level of theory using the Turbomole 6.31 program package,[24] that is, the global hybrid functional B3LYP[25] with 20% of the exact Hartree−Fock exchange admixture, in conjunction with standard Turbomole all-electron def2-TZVP basis sets[26] for all atoms. For the full optimization Grimme's dispersion correction 3 with the Becke−Johnson potential was used.[27] The crystal structures of {**[ECE]Ni−CC−Ph/*ter*Ph→CuBr**} complexes were used as initial structures for full optimization (denoted as "fullopt-D3"). For comparison, partial optimization of only the hydrogen-atom positions for the X-ray-based structure of {**[ECE]-Ni−CC−Ph/*ter*Ph→CuBr**} was also done at the B3LYP/def2-TZVP level (denoted as "crystal/opt-H"). For full optimization of the {**[ECE]Ni−CC−Ph/*ter*Ph**} complexes the optimized structures of {**[ECE]Ni−CC−Ph/*ter*Ph→CuBr**} were taken and the CuBr was removed.

Atomic charges were evaluated at the B3LYP/def2-TZVP level of theory by means of natural population analyses (NPA), using the built-in NBO subroutines of the Gaussian 09 program.[28] Mayer bond orders[29] were evaluated using the program BORDER.[30] The wave functions were also analyzed in the DGrid program[30] by means of the electron localization function (ELF)[31] and the electron localizability indicator based on the parallel-spin electron pair density (ELI-D).[32] For this purpose, the Kohn−Sham orbitals of the (Gaussian 09) single point calculations were transferred to DGrid and the examined property was calculated on a grid with 100 points per bohr. The results of ELF analyses were visualized using the Paraview program.[33]

■ ASSOCIATED CONTENT

Supporting Information

Experimental details for synthesis of organic precursors; NMR, APCI-MS, and XRD experimental data; calculated Mayer bond orders; NPA charges; ELF-D, ELI-D plots; and crystallographic information files in CIF format. This material is available free of charge via the Internet at http://pubs.acs.org.

■ AUTHOR INFORMATION

Corresponding Authors

matthias.driess@tu-berlin.de
jhartwig@berkeley.edu

Author Contributions

[§]D.G. and A.B. contributed equally.

Notes

The authors declare no competing financial interest.

■ ACKNOWLEDGMENTS

Financial support by the Einstein Foundation Berlin and the Cluster of Excellence UniCat (financed by the Deutsche Forschungsgemeinschaft and administered by the TU Berlin) is gratefully acknowledged. A.B. thanks the Deutsche Forschungsgemeinschaft for an initial postdoctoral fellowship to work with J.F.H. (Grant BR 4069/1-1). We also thank the reviewers of the manuscript for helpful comments and suggestions.

■ REFERENCES

(1) Reviews on pincer complexes: (a) Albrecht, M.; van Koten, G. *Angew. Chem.* **2001**, *113*, 3866; *Angew. Chem., Int. Ed.* **2001**, *40*, 3750. (b) van der Boom, M. E.; Milstein, D. *Chem. Rev.* **2003**, *103*, 1759. (c) *The Chemistry of Pincer Compounds*; Morales-Morales, D., Jensen, C. M., Eds.; Elsevier: Amsterdam, 2007. (d) Albrecht, M.; Linder, M. *Dalton Trans.* **2011**, *40*, 8733. (e) Zargarian, D.; Castonguay, A.; Spasyuk, D. M. *Top. Organomet. Chem.* **2013**, *40*, 131.

(2) (a) Zhao, J.; Goldman, A. S.; Hartwig, J. F. *Science* **2005**, *307*, 1080. (b) Morgan, E.; MacLean, D. F.; McDonald, R.; Turculet, L. *J. Am. Chem. Soc.* **2009**, *131*, 14234.

(3) Review on alkane dehydrogenation: Choi, J.; MacArthur, A. H. R.; Brookhart, M.; Goldman, A. S. *Chem. Rev.* **2011**, *111*, 1761.

(4) (a) Eberhard, M. R.; Wang, Z.; Jensen, C. M. *Chem. Commun.* **2002**, 818. (b) Solano-Prado, M. A.; Estudiante-Negrete, F.; Morales-Morales, D. *Polyhedron* **2010**, *29*, 592.

(5) Reviews on group 14 metallylenes: (a) Mizuhata, Y.; Sasamori, T.; Tokitoh, N. *Chem. Rev.* **2009**, *109*, 3479. (b) Mandal, S. K.; Roesky, H. W. *Chem. Commun.* **2010**, *46*, 6016. (c) Yao, S.; Xiong, Y.; Driess, M. *Organometallics* **2011**, *30*, 1748. (d) Asay, M.; Jones, C.; Driess, M. *Chem. Rev.* **2011**, *111*, 354.

(6) Review on metallylene complexes: Blom, B.; Stoelzel, M.; Driess, M. *Chem.—Eur. J.* **2013**, *19*, 40.

(7) Brück, A.; Gallego, D.; Wang, W.; Irran, E.; Driess, M.; Hartwig, J. F. *Angew. Chem., Int. Ed.* **2012**, *51*, 11478; *Angew. Chem.* **2012**, *124*, 11645.

(8) Wang, W.; Inoue, S.; Irran, E.; Driess, M. *Angew. Chem., Int. Ed.* **2012**, *51*, 3691; *Angew. Chem.* **2012**, *124*, 3751.

(9) Reviews about C−C coupling reactions: (a) Hassan, J.; Sévignon, M.; Gozzi, C.; Schulz, E.; Lemaire, M. *Chem. Rev.* **2002**, *102*, 1359. (b) Nicolaou, K. C.; Bulger, P. G.; Sarlah, D. *Angew. Chem., Int. Ed.* **2005**, *44*, 4442. (c) Suzuki, A. *Angew. Chem., Int. Ed.* **2011**, *50*, 6722. (d) Negishi, E.-i. *Angew. Chem., Int. Ed.* **2011**, *50*, 6738. (e) Seechurn, C. C. C. J.; Kitching, M. O.; Thomas, J.; Colacot, T. J.; Snieckus, V. *Angew. Chem., Int. Ed.* **2012**, *51*, 5062.

(10) Reviews on the Sonogashira reaction: (a) Sonogashira, K. In *Handbook of Organopalladium Chemistry for Organic Synthesis*; Negishi, E., de Meijere, A., Eds.; Wiley-Interscience: New York, 2002; p 493. (b) Sonogashira, K. *J. Organomet. Chem.* **2002**, *653*, 46. (c) Tykwinski,

R. R. *Angew. Chem.* **2003**, *115*, 1604; *Angew. Chem., Int. Ed.* **2003**, *42*, 1566. (d) Negishi, E.; Anastasia, L. *Chem. Rev.* **2003**, *103*, 1979. (e) Chinchilla, R.; Nájera, C. *Chem. Rev.* **2007**, *107*, 874. (f) Chinchilla, R.; Nájera, C. *Chem. Soc. Rev.* **2011**, *40*, 5084. Examples using Ni-based catalyst: (g) Wang, L.; Li, P.; Zhang, Y. *Chem. Commun.* **2004**, 514. (h) Beletskaya, I. P.; Latyshev, G. V.; Tsvetkov, A. V.; Lukashev, N. V. *Tetrahedron Lett.* **2003**, *44*, 5011. Relevant example of sulphur−carbon coupling reaction catalyzed by phosphinite Ni pincer complex: (i) Gómez-Benítez, V.; Baldovino-Pantaleón, O.; Herrera-Álvarez, C.; Toscano, R. A.; Morales-Morales, D. *Tetrahedron Lett.* **2006**, *47*, 5059.

(11) Vechorkin, O.; Barmaz, D.; Proust, V.; Hu, X. *J. Am. Chem. Soc.* **2009**, *131*, 12078.

(12) CCDC 942871 (**GeCBrGe**), 942872 (terphenylacetylene), and 942864 ([**GeCGe**]**NiBr**), 942865 ([**SiCSi**]**NiC≡C***ter***Ph−CuBr**), 942866 ([**PCP**]**NiBr**), 942867 ([**SiCSi**]**NiBr**), 942868 ([**SiCSi**]**NiC≡CPh−CuBr**), and 942869 ([**SiCSi**]**NiI**) have supplementary crystallographic data for this paper. These data can be obtained free of charge from The Cambridge Crystallographic Data Centre via www.ccdc.cam.ac.uk/data_request/cif. See Supporting Information for further information.

(13) General procedure for the synthesis of copper phenylcetylides in analogy to the following: Fukatsu, K.; Harada, M.; Hinuma, S.; Ito, Y.; Sasaki, S.; Suzuki, N.; Yasuma, T. Patent EP 1559422 A1, 2005; Takeda Pharmaceutical Company Limited. Osakada, K.; Sakata, R.; Yamamoto, T. *Organometallics* **1997**, *16*, 5354.

(14) Manna, J.; John, K. D.; Hopkins, M. D. *Adv. Organomet. Chem.* **1995**, *38*, 79.

(15) The C≡C triple bond distances are not very indicative of a side-on or end-on coordination mode: Si, 1.213 Å; Ge, 1.222 Å; side-on, 1.207−1.239 Å; end-on, 1.193 Å.[15f] (a) Janssen, M. D.; Köhler, K.; Herres, M.; Dedieu, A.; Smeets, W. J. J.; Spek, A. L.; Grove, D. M.; Lang, H.; van Koten, G. *J. Am. Chem. Soc.* **1996**, *118*, 4817. (b) Lang, H.; Köhler, K.; Rheinwald, G. *Organometallics* **1999**, *18*, 598. (c) Köhler, K.; Eichhorn, J.; Meyer, F.; Vidovic, D. *Organometallics* **2003**, *22*, 4426. (d) Thompson, J. S.; Bradley, A. Z.; Park, K.-H.; Dobbs, K. D.; Marshall, W. *Organometallics* **2006**, *25*, 2712. (e) Dias, H. V. R.; Flores, J. A.; Wu, J.; Kroll, P. *J. Am. Chem. Soc.* **2009**, *131*, 11249. (f) Vechorkin, O.; Godinat, A.; Scopelliti, R.; Hu, X. *Angew. Chem., Int. Ed.* **2011**, *50*, 11777; *Angew. Chem.* **2011**, *123*, 11981. (g) Zhao, N.; Zhang, J.; Ying, Y.; Chen, G.; Zhu, H.; Roesky, H. W. *Organometallics* **2013**, *32*, 762.

(16) (a) Becke, A. D. *J. Chem. Phys.* **1993**, *98*, 5648. (b) Lee, C. T.; Yang, W. T.; Parr, R. G. *Phys. Rev. B* **1988**, *37*, 785. (c) Stephens, P. J.; Devlin, F. J.; Chabalowski, C. F.; Frisch, M. J. *J. Phys. Chem.* **1994**, *98*, 11623.

(17) Weigend, F.; Ahlrichs, R. *Phys. Chem. Chem. Phys.* **2005**, *7*, 3297.

(18) (a) Grimme, S.; Antony, J.; Ehrlich, S.; Krieg, H. *J. Chem. Phys.* **2010**, *132*, 154104. (b) Grimme, S.; Ehrlich, S.; Goerigk, L. *J. Comput. Chem.* **2011**, *32*, 1456.

(19) (a) Becke, A. D.; Edgecombe, K. E. *J. Chem. Phys.* **1990**, *92*, 5397. (b) Savin, A.; Jepsen, O.; Flad, J.; Andersen, O. K.; Preuss, H.; von Schnering, H. G. *Angew. Chem., Int. Ed.* **1992**, *31*, 187; *Angew. Chem.* **1992**, *104*, 186. (c) Kohout, M.; Savin, A. *Int. J. Quantum Chem.* **1996**, *60*, 875.

(20) (a) Kohout, M. *Int. J. Quantum Chem.* **2004**, *97*, 651. (b) Kohout, M.; Pernal, K.; Wagner, F. R.; Grin, Y. *Theor. Chem. Acc.* **2004**, *112*, 453.

(21) Pfirrmann, S.; Limberg, C.; Hoppe, E. *Z. Anorg. Allg. Chem.* **2009**, *635*, 312.

(22) Kajigaeshi, S.; Kakinami, T.; Tokiyama, H.; Hirakawa, T.; Okamoto, T. *Chem. Lett.* **1987**, 627.

(23) Nagendran, S.; Sen, S. S.; Roesky, H. W.; Koley, D.; Grubmüller, H.; Pal, A.; Herbst-Irmer, R. *Organometallics* **2008**, *27*, 5459.

(24) Turbomole, version 6.3.1, a development of University of Karlsruhe and Forschungszentrum Karlsruhe GmbH, 1989−2007, and of Turbomole GmBH since 2007; available from http://www.turbomole.com.

(25) (a) Becke, A. D. *J. Chem. Phys.* **1993**, *98*, 5648. (b) Lee, C. T.; Yang, W. T.; Parr, R. G. *Phys. Rev. B* **1988**, *37*, 785. (c) Stephens, P. J.; Devlin, F. J.; Chabalowski, C. F.; Frisch, M. J. *J. Phys. Chem.* **1994**, *98*, 11623.

(26) Weigend, F.; Ahlrichs, R. *Phys. Chem. Chem. Phys.* **2005**, *7*, 3297.

(27) (a) Grimme, S.; Antony, J.; Ehrlich, S.; Krieg, H. *J. Chem. Phys.* **2010**, *132*, 154104. (b) Grimme, S.; Ehrlich, S.; Goerigk, L. *J. Comput. Chem.* **2011**, *32*, 1456.

(28) Frisch, M. J.; Trucks, G. W.; Schlegel, H. B.; Scuseria, G. E.; Robb, M. A.; Cheeseman, J. R.; Scalmani, G.; Barone, V.; Mennucci, B.; Petersson, G. A.; Nakatsuji, H.; Caricato, M.; Li, X.; Hratchian, H. P.; Izmaylov, A. F.; Bloino, J.; Zheng, G.; Sonnenberg, J. L.; Hada, M.; Ehara, M.; Toyota, K.; Fukuda, R.; Hasegawa, J.; Ishida, M.; Nakajima, T.; Honda, Y.; Kitao, O.; Nakai, H.; Vreven, T.; Montgomery, J. A., Jr.; Peralta, J. E.; Ogliaro, F.; Bearpark, M.; Heyd, J. J.; Brothers, E.; Kudin, K. N.; Staroverov, V. N.; Kobayashi, R.; Normand, J.; Raghavachari, K.; Rendell, A.; Burant, J. C.; Iyengar, S. S.; Tomasi, J.; Cossi, M.; Rega, N.; Millam, J. M.; Klene, M.; Knox, J. E.; Cross, J. B.; Bakken, V.; Adamo, C.; Jaramillo, J.; Gomperts, R.; Stratmann, R. E.; Yazyev, O.; Austin, A. J.; Cammi, R.; Pomelli, C.; Ochterski, J. W.; Martin, R. L.; Morokuma, K.; Zakrzewski, V. G.; Voth, G. A.; Salvador, P.; Dannenberg, J. J.; Dapprich, S.; Daniels, A. D.; Farkas, Ö.; Foresman, J. B.; Ortiz, J. V.; Cioslowski, J.; Fox, D. J. *Gaussian 09*, revision A.02; Gaussian, Inc.: Wallingford CT, 2009.

(29) Mayer, I. *BORDER*, version 1.0; Chemical Research Center, Hungarian Academy of Sciences: Budapest, Hungary, 2005; http://occam.chemres.hu/programs.

(30) Kohout, M. *DGrid*, version 4.6; Radebeul, Germany, 2011.

(31) (a) Becke, A. D.; Edgecombe, K. E. *J. Chem. Phys.* **1990**, *92*, 5397. (b) Savin, A.; Jepsen, O.; Flad, J.; Andersen, O. K.; Preuss, H.; Vonschnering, H. G. *Angew. Chem., Int. Ed.* **1992**, *31*, 187. (c) Kohout, M.; Savin, A. *Int. J. Quantum Chem.* **1996**, *60*, 875.

(32) (a) Kohout, M. *Int. J. Quantum Chem.* **2004**, *97*, 651. (b) Kohout, M.; Pernal, K.; Wagner, F. R.; Grin, Y. *Theor. Chem. Acc.* **2004**, *112*, 453.

(33) *Paraview*, version 3.98.1; Kitware Inc.: Clifton Park, NY, U.S., 2013; http://www.paraview.org.